V International Conference on Particle-based Methods – Fundamentals and Applications
PARTICLES 2017
P. Wriggers, M. Bischoff, E. Oñate, D.R.J. Owen, & T. Zohdi (Eds)

LATTICE BOLTZMANN FLUX SOLVER FOR SIMULATION OF HYPERSONIC FLOWS

Z. X. MENG[1], C. SHU[2], L. M. YANG[3], W. H. ZHANG [4], F. HU[5] AND S. Z. LI[6]

[1] College of Aerospace Science and Engineering, National University of Defense Technology
Changsha, 410073, China
Corresponding author: mengzhuxuan1990@gmail.com
[2] Department of Mechanical Engineering, National University of Singapore
10 Kent Ridge Crescent, Singapore 119260, Singapore
mpeshuc@nus.edu.sg
[3] Department of Mechanical Engineering, National University of Singapore
10 Kent Ridge Crescent, Singapore 17576, Singapore
yangliming_2011@126.com
[4] College of Aerospace Science and Engineering, National University of Defense Technology
Changsha, 410073, China
zhangweihua@nudt.edu.cn
[5] College of Aerospace Science and Engineering, National University of Defense Technology
Changsha, 410073, China
hufan@163.com
[6] College of Aerospace Science and Engineering, National University of Defense Technology
Changsha, 410073, China
Lishengze12@gmail.com

Key words: Non-free parameter D1Q4 model, lattice Boltzmann flux solver, hypersonic flows, finite volume method

Abstract: In this paper, a stable Lattice Boltzmann Flux Solver (LBFS) is proposed for simulation of hypersonic flows. In LBFS, the finite volume method is applied to solve the Navier-Stokes equations. One-dimensional Lattice Boltzmann model is applied to reconstruct the inviscid flux across the cell interface, while the viscous flux is solved by conventional smooth approximation function. The present work extends the existing LBFS to calculate hypersonic flow field on the leeward, which is hard to get convergent results due to extremely low pressure effects in this area. Simulation of a biconics model is studied. It is discovered that the tail area of double cone is related to the maximum Mach number that could be convergent. The larger the diameter of tail area is, the smaller Mach number could be convergent. Hence, the low pressure area behind double cone tail will have large effects during the LBFS simulation of hypersonic flow. Two measurements are applied in this paper to overcome the low pressure problem. The first one is to apply a local block grid refinement method based on the flow conditions for improving the stability. The second is to add a constraint parameter to eliminate negative value and give out a proper one. Hence, LBFS is able to get convergent result of the hypersonic flow field on both windward and leeward. Several numerical examples are tested to compare the performance of method presented in this paper. Simulation results show that method present in this paper is able to calculate hypersonic flow field on the leeward with both fine accurate and efficient.

1 INTRODUCTION

The hypersonic flow field is a research focus with its special characteristics [1]: (1) strong shock effect will cause fierce compression after the shock wave, (2) viscosity greatly changed from wall surface to far field area, (3) for hypersonic vehicles flying in high altitude, continuous medium assumption is no longer appropriate because of low density effect. The computational fluid dynamics (CFD) is becoming more and more popular in simulating hypersonic flow field. The finite volume method (FVM) is widely used in existing numerical methods [2]. This largely attributes to its spatial discretization is carried out directly in the physical space. Hence, structural grid is suitable for discretization, which provides an effective way for solving complex geometry problems. In the process of solving N-S equations by FVM, flux solver is the key to evaluate viscous and invicid fluxes at cell interface. The viscous flux is evaluated by applying a smooth function approximation and inviscid flux is calculated by various upwind schemes such as Roe scheme [3], van Leer scheme [4] and AUSM (Advection Upstream Splitting Method) scheme [5].

Boltzmann equation-based method is an alternative approach for simulating compressible flow field, including DVBE [6][8] (discrete velocity Boltzmann equation) and gas-kinetic scheme [9]-[13]. Gas-kinetic scheme have better efficiency than DVBE method. However, both of them are less efficient and more complicated than conventional Navier- Stocks slovers.

Lattice Boltzmann Flux Solver (LBFS) is a more efficient method which is proposed by Ji et al. [14] and for simulating inviscid flows. LBFS is improved by Shu and Yang et al. [15]-[19] and has been proved catching strong shock wave and expansion wave very well. In LBFS, Euler equations are discretized by FVM and the inviscid flux at cell interface is reconstructed by local solution of 1-D compressible Lattice Boltzmann model. LBFS is more efficient and easy to apply than DVBE and gas-kinetic method due to only 1-D Lattice Boltzmann model is applied and macroscopic governing equations are solved. However, because of 1-D model is applied along normal direction at cell interface, the tangential effect cannot be properly considered. Viscous flux should be taken into account to solve viscous problems. From chapman-Enskog expansion analysis [19], the inviscid flux can be fully determined by equilibrium non-equilibrium distribution function at cell interface, and the non-equilibrium part can be treated as numerical dissipation. For compressible viscous flows, especially for hypersonic flows, the numerical dissipation should be controlled. A switch function is proposed by Yang et al. [20] to weight viscous numerical dissipation and has been proved performed well in viscous simulation. For hypersonic flow field, physical values such as pressure in leeward side can be extremely low. Hence it is very easy to get a negative value in calculating process, which make it very difficult to get a convergent result.

In this work, a stable LBFS is proposed for simulation of 2-D compressible hypersonic viscous flows. The inviscid flux is calculated by LBFS and viscous flux is computed by smooth function approximation. Multiblock grids and local grid refinement method are applied to improve calculation stability. Also a constraint parameter is added to eliminate negative value and give out a proper one in calculating process. Besides, the implicit LU-SGS method is used to speed up the convergence rate. In the end, a biconics model in Ma=9.86 flow field is simulated to validate the developed solver. The results of solver presented in this work is compared with van Leer and Roe scheme to evaluate the precision proposed in this article.

2 METHODOLOGY

In LBFS, Navier-Stockes equations are solved in macroscopic scale and local solution of Lattice Boltzmann equations are applied in to construct inviscid flux solver at the cell interface. It has been proved that particle potential energy is independent from lattice velocity [15]. Lattice velocity would be decided by higher momentum conservation relation in this work instead of by artificial selection in traditional method.

N-S equations of intergral form without source term can be written as following.

$$\frac{\partial}{\partial t}\int_{\Omega}\mathbf{W}d\Omega+\oint_{\Gamma}(\mathbf{F}_c-\mathbf{F}_v)ds=0 \tag{1}$$

In which the conservative variables $\mathbf{W}$, inviscid flux $\mathbf{F}_c$ and viscous flux $\mathbf{F}_v$ are given by Eq. (2) in 2-D flow field.

$$\mathbf{W}=\begin{bmatrix}\rho\\ \rho u\\ \rho v\\ \rho E\end{bmatrix},\ \mathbf{F}_c=\begin{bmatrix}\rho U_n\\ \rho u U_n+n_x p\\ \rho v U_n+n_y p\\ (\rho E+p)U_n\end{bmatrix},\ \mathbf{F}_v=\begin{bmatrix}0\\ n_x\tau_{xx}+n_y\tau_{xy}\\ n_x\tau_{yx}+n_y\tau_{yy}\\ n_x\Theta_x+n_y\Theta_y\end{bmatrix} \tag{2}$$

The expressions of normal velocity U_n and total energy E are shown as Eq. (3). Where $e=p/[(\gamma-1)\rho]$ is the potential energy of mean flow.

$$\begin{aligned}U_n&=n_x u+n_y v\\ E&=e+\frac{1}{2}(u^2+v^2)\end{aligned} \tag{3}$$

The integral of fluxes in Eq. (1) can be discretized by FVM and the approximated summation form can be written as

$$\frac{d\mathbf{W}_I}{dt}=-\frac{1}{\Omega_I}\sum_{i=1}^{N_f}(F_{ci}-F_{vi})S_i \tag{4}$$

In which I represents the control volume index, Ω_I is the volume and N_f is number of faces of control volume I. In this paper, the inviscid flux F_c in Eq. (4) will be solved by LBFS with non-free parameter D1Q4 model [18] and viscous flux F_v will be solved by central difference method.

2.1 Non-free parameter D1Q4 lattice Boltzmann model

The distribution of discrete lattice velocities for D1Q4 model is shown in Fig. 1. This model contains 4 equilibrium distribution functions f_1^{eq}, f_2^{eq}, f_3^{eq}, f_4^{eq} and 2 lattice velocities d_1, d_2 (shown as Eq. (5)). The derivation process details are shown in references [18] .

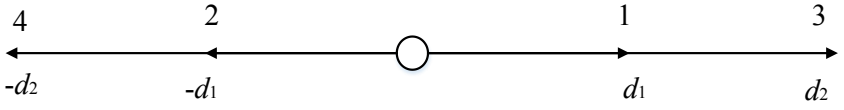

Figure 1: Distribution of discrete lattice velocities for D1Q4 model

$$
\begin{aligned}
f_1^{eq} &= \frac{\rho(-d_1 d_2^2 - d_2^2 u + d_1 u^2 + d_1 c^2 + u^3 + 3uc^2)}{2d_1(d_1^2 - d_2^2)} \\
f_2^{eq} &= \frac{\rho(-d_1 d_2^2 + d_2^2 u + d_1 u^2 + d_1 c^2 - u^3 - 3uc^2)}{2d_1(d_1^2 - d_2^2)} \\
f_3^{eq} &= \frac{\rho(d_1^2 d_2 + d_1^2 u - d_2 u^2 - d_1 c^2 - u^3 - 3uc^2)}{2d_2(d_1^2 - d_2^2)} \\
f_4^{eq} &= \frac{\rho(d_1^2 d_2 - d_1^2 u - d_2 u^2 - d_2 c^2 + u^3 + 3uc^2)}{2d_2(d_1^2 - d_2^2)} \\
d_1 &= \sqrt{u^2 + 3c^2 - \sqrt{4u^2 c^2 + 6c^4}} \\
d_2 &= \sqrt{u^2 + 3c^2 + \sqrt{4u^2 c^2 + 6c^4}}
\end{aligned}
\tag{5}
$$

In which $c = \sqrt{Dp/\rho}$ represents particular velocity of particles and D is space dimension. It has been proved by Yang [18] that physical conservation laws (Eq. (6)) can revivify the N-S equations by applying relations in Eq. (5). ξ_i means particle velocity in *i*-direction, for example $\xi_1 = d_1, \xi_2 = -d_1, \xi_3 = d_2$ and $\xi_4 = -d_2$. For higher dimensional problems, the D1Q4 model should be applied along the normal direction of cell interface [18] as is shown in Fig. 2 of the 2D case. The normal velocity U_n (Eq. (3)) and tangential velocity $U_\tau = (u_{\tau x}, u_{\tau y}) = \mathbf{u} - U_n \mathbf{n}$ in Fig. 2 will replace u in Eq. (6). Finally, we will get $u = U_n n_x + u_{\tau x}$.

$$
\begin{aligned}
\rho &= \sum_{i=1}^{4} f_i^{eq} \\
\rho u &= \sum_{i=1}^{4} f_i^{eq} \xi_i \\
\rho u^2 + \rho c^2 &= \sum_{i=1}^{4} f_i^{eq} \xi_i \xi_i \\
\rho u^3 + 3\rho u c^2 &= \sum_{i=1}^{4} f_i^{eq} \xi_i \xi_i \xi_i
\end{aligned}
\tag{6}
$$

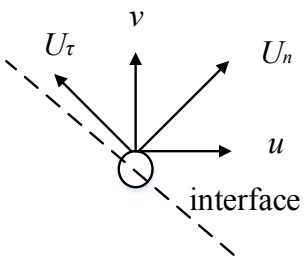

Figure 2: Application of 1D model to 2D case

By applying Eq. (6) to Eq. (2), we will get the conservation variable $\mathbf{W}$ and inviscid flux $\mathbf{F}_c$

of 2-D flow field as following.

$$\mathbf{W}=\begin{bmatrix}\rho\\ \rho(U_n n_x+u_{\tau x})\\ \rho(U_n n_y+u_{\tau y})\\ \rho(U_n^2/2+e)+\rho|U_\tau|^2/2\end{bmatrix},\ \mathbf{F}_c=\begin{bmatrix}\rho U_n\\ \rho(U_n^2+p)n_x+\rho U_n u_{\tau x}\\ \rho(U_n^2+p)n_y+\rho U_n u_{\tau y}\\ (\rho(U_n^2/2+e)+p)U_n+\rho|U_\tau|^2/2\end{bmatrix} \tag{7}$$

2.2 Inviscid flux model

Suppose that cell interface is located at $x_{c,j+1/2}=0$, then the inviscid flux at interface $\overline{\mathbf{F}}_c$ is decided by normal velocity and can be written as Eq. (8). In which the moments $\boldsymbol{\varphi}_a=\left[1,\xi_i,\xi_i^2/2+e_p\right]^T$ and $f_i(0,t)$ is the distribution function at cell interface. Generally speaking. $f_i(0,t)$ is summation of equilibrium part $f_i^{eq}(0,t)$ and non equilibrium part $f_i^{neq}(0,t)$.

$$\overline{\mathbf{F}_c}=\begin{bmatrix}\rho U_n\\ \rho U_n^2+p\\ (\rho(U_n^2/2+e)+p)U_n\end{bmatrix}=\sum_{i=1}^{4}\xi_i\boldsymbol{\varphi}_a f_i(0,t) \tag{8}$$

To recover N-S equations by Boltzmann equation from Chapman-Enskog analysis [19][21][22][23][24], the non-equilibrium part $f_i^{neq}(0,t)$ can be written as following.

$$f_i^{neq}(0,t)=-\tau\left(\frac{\partial f_i}{\partial t}+\xi_i\frac{\partial f_i}{\partial x}\right)\Bigg|_{(0,t)} \tag{9}$$

Then applying Taylor series expansion in tome and physics space, Eq. (9) can be simplified as following.

$$f_i^{neq}(0,t)=-\frac{\tau}{\delta t}\left[f_i(0,t)-f_i(-\xi_i\delta t,t-\delta t)\right]+o(\delta t) \tag{10}$$

At the cell interface the equillibrium distribution function is $f_i(0,t)=f_i^{eq}(0,t)$. $f_i(-\xi_i\delta t,t-\delta t)$ is equilibrium distribution function at surrouding point of the cell interface. Substituting Eq. (9) into Eq. (8) as following.

$$f_i(0,t)=f_i^{eq}(0,t)-\tau_0\left[f_i(0,t)-f_i(-\xi_i\delta t,t-\delta t)\right]+o(\delta t) \tag{11}$$

In which $\tau_0=\tau/\delta t$ is the dimensionless collision time and δt dt is the streaming time step and represents the physical viscous of N-S equations. The contribution of non-equlibrium part is always treated as numerical dissipation in LBFS. Therefore, τ_0 can be regarded as the weight of numerical dissipation. We have $\tau_0=\max\left\{\tau^L,\tau^R\right\}$ in this work. In which $\tau^L=\max_{j=1,N_{fL}}\left\{\tau_j\right\},\tau^R=\max_{j=1,N_{fR}}\left\{\tau_j\right\}$ and $,\tau_j=\tanh\left(C\frac{\left|p^L-p^R\right|}{p^L+p^R}\right)$. N_{fL} and N_{fR} are the number of control volume on left and right side of cell interface. The details can be found in [25].

Substituting Eq. (11) into Eq. (8) we will get inviscid flux $\overline{\mathbf{F}}_c$ which is decided by tangential velocity as following.

$$\begin{aligned}\overline{\mathbf{F}}_c &= \sum_{i=1}^{4}\xi_i\boldsymbol{\varphi}_a f_i(0,t)+\tau_0\left[\sum_{i=1}^{4}\xi_i\boldsymbol{\varphi}_a f_i(-\xi_i\delta t,t-\delta t)-\sum_{i=1}^{4}\xi_i\boldsymbol{\varphi}_a f_i(0,t)\right] \\ &= \overline{\mathbf{F}}_c^{\mathrm{I}}+\tau_0(\overline{\mathbf{F}}_c^{\mathrm{II}}-\overline{\mathbf{F}}_c^{\mathrm{I}})\end{aligned} \tag{12}$$

Total invisicid flux at cell interface considering tangential velocity contribution is shown as following.

$$\mathbf{F}_c = \mathbf{F}_c^{\mathrm{I}}+\tau_0(\mathbf{F}_c^{\mathrm{II}}-\mathbf{F}_c^{\mathrm{I}}) \tag{13}$$

$\mathbf{F}_c^{\mathrm{I}}$ represents contribution of equilibrium distribution function $f_i^{eq}(0,t)$ at cell interface and $\mathbf{F}_c^{\mathrm{II}}$ means equilibrium distribution function $f_i(-\xi_i\delta t,t-\delta t)$ at surrouding point of the cell interface.

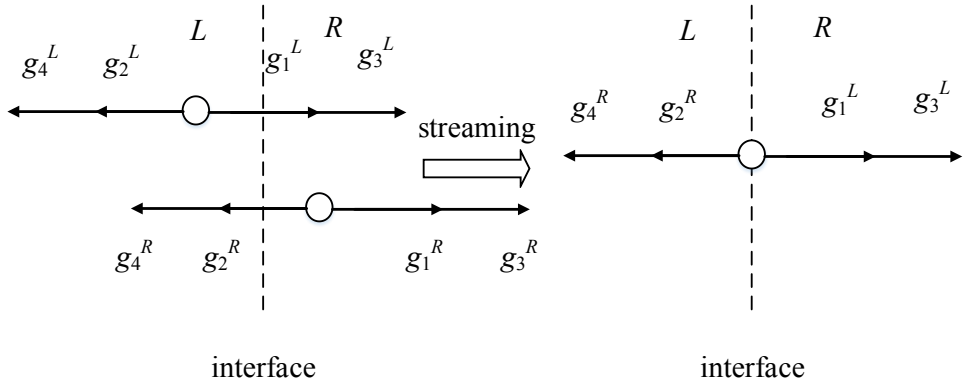

Figure 3: Streaming process based on D1Q4 model at cell interface

Supposing that a local Riemann problem is formed at cell interface, which is shown in Fig. 3. Hence, equilibrium distribution function $f_i(-\xi_i\delta t,t-\delta t)$ at surrouding point of cell interface can be decided by the location of $-\xi_i\delta t$, which is shown as Eq. (14).

$$f_i(-\xi_i\delta t,t-\delta t)=\begin{cases}f_i^L & -\xi_i\delta t\le 0\\ f_i^R & -\xi_i\delta t>0\end{cases} \tag{14}$$

More specifically, Eq. (14) can be written as following for D1Q4 model.

$$f_i(-\xi_i\delta t,t-\delta t)=\begin{cases}f_i^L & i=1,3\\ f_i^R & i=2,4\end{cases} \tag{15}$$

By applying the relationship of $f_i(0,t)=f_i^{eq}(0,t)-f_i^{neq}(0,t)$, the conservation flux which is decided by tangential velocity can be written as following.

$$\overline{\mathbf{W}}^M=\begin{bmatrix}\rho\\ \rho U_n\\ \rho(U_n^2/2+e)\end{bmatrix}=\sum_{i=1}^{4}\boldsymbol{\varphi}_a f_i^{eq}(0,t)+\sum_{i=1}^{4}\boldsymbol{\varphi}_a f_i^{neq}(0,t) \tag{16}$$

The subscript M means parameter on cell interface. The non-equilibrium part has no contribution to calculate conservation variables according to the compatibility condition [19], which is shown as following.

$$\sum_{i=1}^{4}\boldsymbol{\varphi}_a f_i^{neq}(0,t) = -\tau_0\sum_{i=1}^{4}\boldsymbol{\varphi}_a\left[f_i(0,t) - f_i(-\xi_i\delta t, t-\delta t)\right] = 0 \tag{17}$$

Substituting Eq.(17) into Eq. (16) we will get

$$\overline{\mathbf{W}}^M = \sum_{i=1}^{4}\boldsymbol{\varphi}_a f_i(0,t) = \sum_{i=1}^{4}\boldsymbol{\varphi}_a f_i(-\xi_i\delta t, t-\delta t) \tag{18}$$

By applying Eq. (15) into Eq. (18), the conservation flux which is decided by tangential velocity $\overline{\mathbf{W}}^M$ can be written as

$$\overline{\mathbf{W}}^M = \sum_{i=1,3}\boldsymbol{\varphi}_a f_i^L + \sum_{i=2,4}\boldsymbol{\varphi}_a f_i^R \tag{19}$$

Therefore, density, normal velocity and pressure at cell interface are obtained from Eq. (19). Then the tangential velocity at cell interface can be calculated by the following equation.

$$(\rho U_\tau)^M = \sum_{i=1,3} f_i^L U_\tau^L + \sum_{i=2,4} f_i^R U_\tau^R \tag{20}$$

In which U_τ^M, U_τ^L and U_τ^R are tangential velocity at cell interface, on the left and right side of cell interface respectively. Based on Eq. (19) and Eq. (20), all variables at cell interface such as ρ^M, p^M U_τ^M and U_n^M can be obtained. Substituting these variables to Eq. (5) and we can get the equlibrium distibution function $f_i(0,t)$ at cell interface.

The $\mathbf{F}_c^{\mathrm{I}}$ in Eq. (13) including two parts, which are $\overline{\mathbf{F}}_c^{\mathrm{I}}$ decided by normal velocity and the part decided by tangential velocity. Then $\mathbf{F}_c^{\mathrm{I}}$ can be written as following by applying variables at cell interface.

$$\mathbf{F}_c^{\mathrm{I}} = \begin{bmatrix} \rho U_n \\ (\rho U_n^2 + p)n_x + \rho U_n u_{\tau x} \\ (\rho U_n^2 + p)n_y + \rho U_n u_{\tau y} \\ (\rho({U_n}^2/2 + e) + p)U_n + \rho U_n \left|U_\tau\right|^2/2 \end{bmatrix} \tag{21}$$

Also $\mathbf{F}_c^{\mathrm{II}}$ is consists of $\overline{\mathbf{F}}_c^{\mathrm{II}}$ decided by normal velocity and the part decided by tangential velocity. Substituting equilibrium distribution function $f_i(-\xi_i\delta t, t-\delta t)$ at surrouding point of cell interface to Eq. (8) we will get $\overline{\mathbf{F}}_c^{\mathrm{II}}$ as following.

$$\overline{\mathbf{F}}_c^{\mathrm{II}} = \sum_{i=1,3}\xi_i\boldsymbol{\varphi}_\alpha f_i^L + \sum_{i=2,4}\xi_i\boldsymbol{\varphi}_\alpha f_i^R \tag{22}$$

Then the tangential velocity at cell interface can be calculated by the following equation.

$$
\begin{aligned}
(\rho U_n U_\tau)^M &= \sum_{i=1,3} \xi_i f_i^L U_\tau^L + \sum_{i=2,4} \xi_i f_i^R U_\tau^R \\
(\rho U_n |U_\tau|^2)^M &= \sum_{i=1,3} \xi_i f_i^L |U_\tau^L|^2 + \sum_{i=2,4} \xi_i f_i^R |U_\tau^R|^2
\end{aligned}
\tag{23}
$$

Now $\mathbf{F}_c^{\mathrm{II}}$ can be expressed as following. In which $f_i = f_i(-\xi_i \delta t, t - \delta t)$.

$$
\mathbf{F}_c^{\mathrm{II}} = \begin{bmatrix}
\sum_{i=1}^{4} \xi_i f_i \\
\sum_{i=1}^{4} \xi_i \xi_i f_i \bullet n_x + \sum_{i=1}^{4} \xi_i f_i \bullet U_{\tau x}^M \\
\sum_{i=1}^{4} \xi_i \xi_i f_i \bullet n_y + \sum_{i=1}^{4} \xi_i f_i \bullet U_{\tau y}^M \\
\sum_{i=1}^{4} \xi_i (\frac{1}{2} \xi_i \xi_i + e_p) f_i + \frac{1}{2} \sum_{i=1}^{4} \xi_i f_i \bullet |U_\tau^M|^2
\end{bmatrix}
\tag{24}
$$

By substituting Eq. (21) and Eq. (24) to Eq. (13) we get inviscid flux $\mathbf{F}_c$ on cell interface.

2.3 Viscous flux model

In this work, central difference scheme is applied to solve the visous flux $\mathbf{F}_v$. Stress tensor $\overline{\overline{\tau}}$ and flux vector Θ in Eq. (2) are given by

$$
\begin{aligned}
\overline{\overline{\tau}} &= \mu \left[\left(\nabla \mathbf{u} + (\nabla \mathbf{u})^T \right) - \frac{2}{3} (\nabla \bullet \mathbf{u}) \overline{\overline{\mathbf{I}}} \right] \\
\Theta &= \overline{\overline{\tau}} \bullet \mathbf{u} + k \nabla T
\end{aligned}
\tag{25}
$$

In which μ is dynamic viscosity and decided by Sutherland's law and turbulence model. k is thermal conductivity and $\overline{\overline{\mathbf{I}}}$ is unit matrix.

For physical variables on cell interface, such as u, v, w and k, can be calculated by arithmetic mean value on left and right side of cell interface, shown as following.

$$
\phi^M = \frac{1}{2} (\phi^L + \phi^R)
\tag{26}
$$

Where ϕ represents any physical variables. The derivatives in Eq. (25) are calculated by finite difference scheme and detils are shwon in reference [26].

2.4 Method to improve numerical stability

Multiblock grids are applied to refine local grid quality. Grids local refinement method is used near wall surface and block interface. Hence, scheme stablity has been improved by reducing spatial step, especially in the leeward side of flow field. Besides, a constraint judgement is added in our code to avoid negative value in calculating process. In this work, implicit LU-SGS method [27] is applied to speed up the convergence rate and keep calculation robust.

3 NUMERICAL SIMULATION

Biconics model is used to verify the present solver. The shape of biconics model is shown as Fig. 4. The head curvature radius is 3.84mm, semi-cone angle is 12.84 degree in front and 7 degree in back, while the length of front cone is 69.55mm and 122.24mm totally. The free stream has a pressure of $P_\infty = 59.92\text{Pa}$, temperature of $T_\infty = 48.88\text{K}$ and Mach number $Ma_\infty = 9.86$.

Fig. 5 shows mach number distribution obtained by present solver in this article. It can be seen clearly that LBFS can capture strong shock waves and flow inside the boundary layer exactly. The maximum Mach number is 16.93Ma.

Fig. 6 shows the pressure contours bibonics model without tail flow field, and Fig. 7 is the one has tail field. Fig. 8 and Fig. 9 show temperature distributions. One block grids are applied of flow field without tail simulation. It is easier for calculation convergent without low pressure effect in back tail flow.

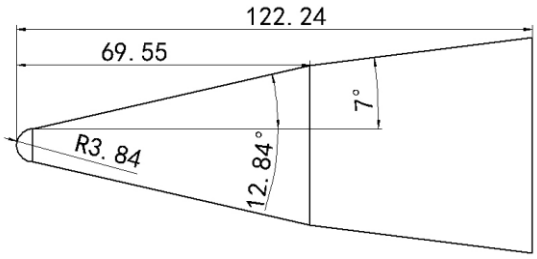

Figure 4: Measurements of biconics model

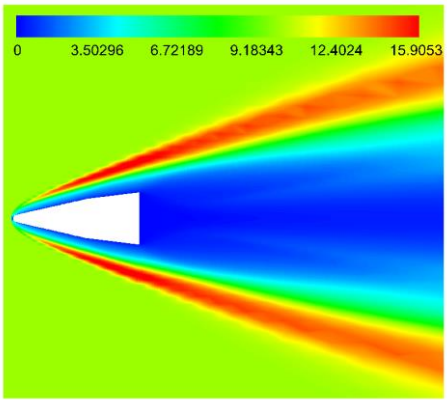

Figure 5: Mach number contours obtained by LBFS at Ma=9.86

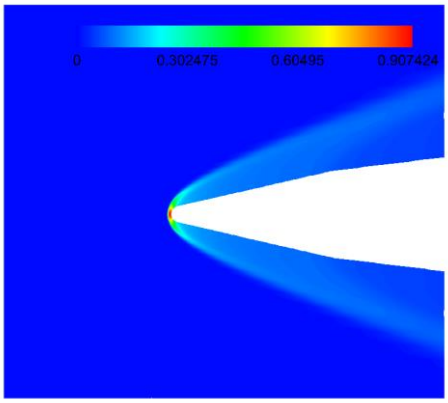

Figure 6: Pressure contours obtained by LBFS without back tail flow field

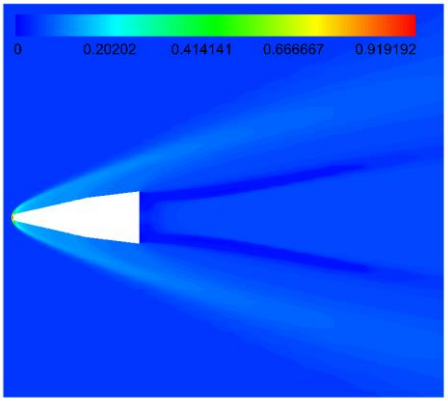

Figure 7: Pressure contours obtained by LBFS with back tail flow field

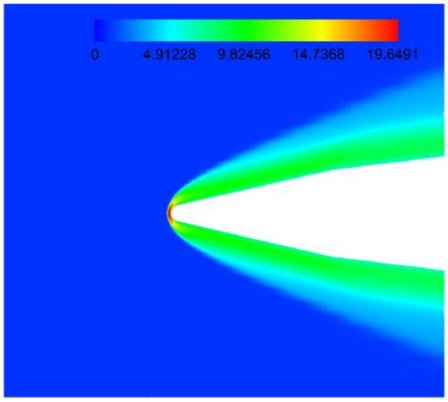

Figure 8: Temperature contours obtained by LBFS without back tail flow field

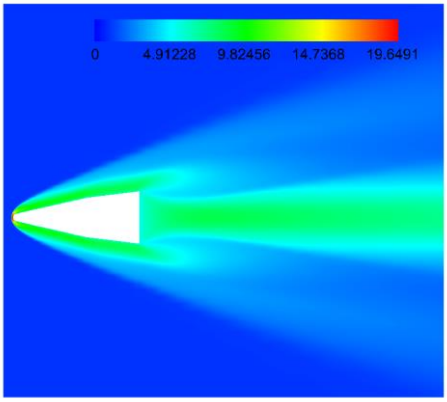

Figure 9: Temperature contours obtained by LBFS with back tail flow field

The hypersonic flow can only be affected by inflow in theory. To validate this we give out comparision of results in with and without back tail flow field which are shown as Fig. 10 and Fig. 11. Fig. 10 is comparison of pressure coefficient Cp. Results of with back tail flow field are shown by lines and without tail results are shown by symbols. Also to evaluate LBFS in this work, van Leer scheme and Roe scheme are applied and the results are shown below. Because high temperature is a focous problem in hypersonic flow research, we also discuss heat flux calculation here. Fig. 11 gives out comparison of heat flux. The experiment data is from reference [28].

Results in Fig. 10 and Fig. 11 show that LBFS in this work can offer both high computational accuracy and numerical stablity. Hence, it is demonstrated useful for aircraft research and design.

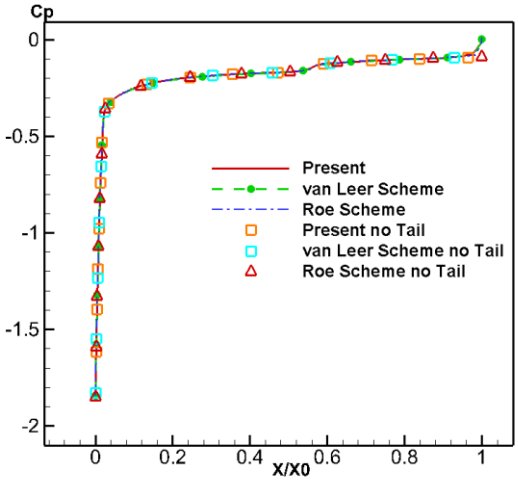

Figure 10: Cp comparison of biconics model between different methods

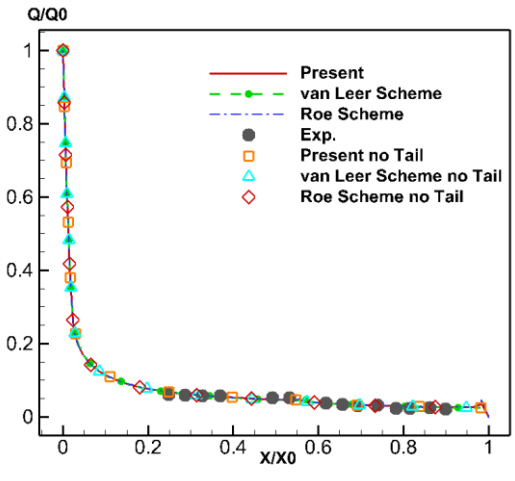

Figure 11: Heat flux ratio comparison of biconics model between different methods

4 CONCLUSIONS

This paper presents a stable lattice Boltzmann flux solver (LBFS) for simulation of 2-D compressible hypersonic viscous flows. The present work is a new application which make it possible for simulation in flow field of leeward wall surface. Physical values in leeward side can be extremely low in hypersonic flows due to strong shock effect. Negative values are easy exsting in calculating process. Hence, multiblock grids and local grid refinement method are applied to promise the calculation convergency. And we have added a constraint parameter to eliminate negative value in calculating process.

Numerical simulation of a biconics model in Ma=9.86 is used to validate the developed solver. The results comparison of solver presented in this work, van Leer and Roe scheme show that method presented in this work have high computational accuracy and stablity.

5 ACKONWLEDGMENT

The authors would like to appreciate Dr. Xinliang Li (Institute of Mechanics of Chinese Academy of Sciences) for his kindly help in programming our 2D Navier-Stokes code.

REFERENCES

[1] J. D. Anderson, Hypersonic and High Temperature Gas Dynamics. McGraw-Hill, 1989.
[2] J. Blazek, Principle and Application, Computation Fluid Dynamics, Elsevier, 2001.
[3] P. L. ROE, Approximate Riemann solvers, parameter vectors, and difference schemes, J. Comput.Phys., 43 (1981), pp. 357–372.
[4] B. VAN LEER, Flux vector splitting for the Euler equations, Lecture Notes in Physics, 170 (1982), pp. 507–512.
[5] M. S. LIOU AND C. J. STEFFEN, A new flux splitting scheme, J. Comput. Phys., 107 (1993), pp. 23–39.
[6] T. Kataoka, M. Tsutahara, Lattice Boltzmann method for the compressible Navier-Stokes equations with flexible specific-heat ratio, Phys. Rev. E, 69 (2004), R035701.
[7] K. Qu, C. Shu, Y.T. Chew, Alternative method to construct equilibrium distribution functions in lattice-Boltzmann method simulation of inviscid compressible flows at high Mach number, Phys. Rev. E, 75 (2007), 036706.
[8] Q. Li, Y.L. He, Y. Wang, W.Q. Tao, Coupled double-distribution-function lattice Boltzmann method for the compressible Navier-Stokes equations, Phys. Rev. E, 76 (2007), 056705.
[9] D. Chae, C. Kim, O.H. Rho, Development of an improved gas-kinetic BGK scheme for inviscid and viscous flows, J. Comput. Phys., 158 (2000), 1-27.
[10] K. Xu, A gas-kinetic BGK scheme for the Navier-Stocks equations and its connection with artificial dissipation and Godunov method, J. Comput. Phys., 171 (2001), 289-335.
[11] J. Jiang, Y.H. Qian, Implicit gas-kinetic BGK scheme with multigrid for 3D stationary transonic high-Reynolds number flows, Comput. Fluids, 66 (2012), 21-28.
[12] S.Z. Chen, K. Xu, C.B. Lee, Q.D. Cai, A unified gas kinetic scheme with moving mesh and velocity space adaptation, J. Comput. Phys., 231 (2012), 6643-6664.
[13] L.M. Yang, C. Shu, J. Wu, N. Zhao, Z.L. Lu, Circular function-based gas-kinetic scheme for simulation of inviscid compressible flows, J. Comput. Phys., 255 (2013), 540-557.
[14] C. Z. JI, C. SHU AND N. ZHAO, A lattice Boltzmann method-based flux solver and its

application to solve shock tube problem, Mod. Phys. Lett. B., 23 (2009), pp. 313–316.
[15] L. M. YANG, C. SHU AND J. WU, Development and comparative studies of three non-free parameter lattice Boltzmann models for simulation of compressible flows, Adv. Appl. Math. Mech., 4(2012), pp. 454–472.
[16] L. M. YANG, C. SHU AND J. WU, A moment conservation-based non-free parameter compressible lattice Boltzmann model and its application for flux evaluation at cell interface, Comput. Fluids, 79 (2013), pp. 190–199.
[17] C. SHU, Y. WANG, L. M. YANG AND J. WU, Lattice Boltzmann flux solver: an efficient approach for numerical simulation of fluid flows, Transactions of Nanjing University of Aeronautics and Astronautics, 31 (2014), pp. 1–15.
[18] L. M. YANG, Research on Compressible Lattice Boltzmann Model and Simplified Distribution Function-Based Flux Solver, Nanjing University of Aeronautics and Astronautics, 2016.
[19] Z.L. Guo and C. Shu, Lattice Boltzmann method and its applications in engineering, World Scientific Publishing, 2013.
[20] L.M. Yang, C. Shu, J. Wu., Extension of lattice Boltzmann flux solver for simulation of 3D viscous compressible flows, Computers and Mathematics with Application, 71 (2016): 2069-2081.
[21] R. BENZI, S. SUCCI AND M. VERGASSOLA, The lattice Boltzmann equation: theory and application,Physics Report, 1992.
[22] P. L. BHATNAGAR, E. P. GROSS AND M. KROOK, A model for collision processes in gases. I:small amplitude processes in charged and neutral one-component systems, Phys. Rev., 94 (1954),pp. 511–525.
[23] K. XU AND X. Y. HE, Lattice Boltzmann method and gas-kinetic BGK scheme in the low-Machnumber viscous flow simulations, J. Comput. Phys., 190 (2003), pp. 100–117.
[24] L.M. Yang, C. Shu, J. Wu. A hybrid lattice Boltzmann flux solver for simulation of viscous compressible flows. Adv. Appl. Math. Mech., 2016, 8(6): 887-910.
[25] L.M. Yang, C. Shu, J. Wu. A three-dimensional explicit sphere function-based gas-kinetic flux solver for simulation of inviscid compressible flows. Journal of Computational Physics, 295 (2015), 322-339.
[26] R.C. Swanson, R. Radespiel, Cell centered and cell vertex multigrid schemes for the Navier-Stokes equations, AIAA Journal, 29 (1991) 697-703.
[27] X. L. Li, D. X. Fu, Y. W. Ma, Direct numerical simulation of compressible turbulent flows, Acta Mech Sin, 26 (2010), 795-806.
[28] Miller C G. Experimental and predicted heating distributions for biconics at incidence in air at Mach 10[R].NASA-TP-2334, 1984.